4-2022

A RAPID SPECIES-SPECIFIC DIAGNOSTIC ASSAY FOR XYLARIA NECROPHORA, THE PATHOGEN BEHIND TAPROOT DECLINE OF SOYBEAN IN THE SOUTHERN UNITED STATES

Sophie Baron Sheffield

A RAPID SPECIES-SPECIFIC DIAGNOSTIC ASSAY FOR *XYLARIA NECROPHORA*, THE PATHOGEN BEHIND TAPROOT DECLINE OF SOYBEAN IN THE SOUTHERN UNITED STATES

by

Sophie Baron Sheffield

Undergraduate honors thesis under the direction of

Dr. Vinson Doyle

Department of Plant Pathology and Crop Physiology

Submitted to the LSU Roger Hadfield Ogden Honors College in partial fulfillment of the Upper Division Honors Program.

April 2022

Louisiana State University
& Agricultural and Mechanical College
Baton Rouge, Louisiana

ABSTRACT

Xylaria necrophora, the fungal pathogen behind taproot decline of soybean (TRD) in the southern United States, is undetectable prior to planting and lengthy to diagnose once soybean is infected. Diagnostics of TRD mostly rely on recognition of the foliar and root symptoms, described as interveinal chlorosis followed by necrosis on leaves, and necrosis along the main root. To provide an alternative diagnostic method for the rapid detection of *X. necrophora* in plant and soil samples, we developed a sensitive species-specific molecular assay. In previous studies, priming regions specific to *X. necrophora* were detected using the Rapid identification of PCR primer pairs Unique Core Sequences (RUCS) program and validated by PCR amplification of the target regions. Once we confirmed specific amplification of *X. necrophora* DNA with the RUCS primer pairs, we designed a corresponding quantitative real-time PCR (qPCR) protocol with a FAM-TAMRA probe. We used serial dilutions of *X. necrophora* DNA and off-target fungal DNA extracted from pure cultures to validate the qPCR protocol and calculate a standard curve equation of cycle threshold and log DNA concentration. The minimum target DNA detected by the assay was 0.000256 ng at a mean cycle threshold of 36.0. We empirically tested the diagnostic assay on DNA extracted from: (1) 2.5-year-old field-collected fungal, soybean debris, and associated soil samples, (2) recent field-collected soybean debris and associated soil samples from areas of low, moderate, and high levels of TRD, and (3) lab-inoculated plant and associated soil samples. However, amplification sometimes does not occur in infected samples; this may be due to the presence of PCR inhibitors or a lack of sufficient target DNA in the samples. This assay provides rapid species-specific amplification of *X. necrophora* with high sensitivity, useful for diagnostic purposes. Furthermore, this assay can be used in epidemiological studies aimed to better understand the spread and distribution of the pathogen in the environment.

INTRODUCTION

Taproot decline of soybean (TRD) is an emerging disease in the southern United States caused by a fungal pathogen, *Xylaria necrophora* (Garcia-Aroca et al. 2021). TRD is characterized by interveinal chlorosis followed by necrosis on leaves and by black, charcoal-like stomatal tissue on roots (Allen et al. 2017). TRD is often misdiagnosed because similar symptoms are caused by other fungal diseases of soybean, such as sudden death syndrome caused by *Fusarium virguliforme* (=*Neocosmophora phaseoli*, =*Fusarium solani*) (Aoki et al. 2005; Hartman et al. 2004; Chang et al. 2015; O'Donnell et al. 2020) or black root rot caused by caused by *Thielaviopsis basicola* (Allen et al. 2017). The current diagnostic process for TRD is lengthy and relies on assessments of foliar and root symptoms in soybean, which may not always be visible. The pathogen must then be isolated from the soybean plant and identified through amplification of one or more molecular markers, sequencing, and phylogenetic analyses (Squiers 2021).

A widely used test to quickly identify the presence of DNA of an organism without sequencing and running phylogenetic analyses is real-time PCR, or quantitative polymerase chain reaction (qPCR) (Higuchi et al. 1993). qPCR can be used to amplify and quantify target DNA in real-time (Kralik and Ricchi 2017), whereas regular PCR can only confirm the presence or absence of target DNA in a sample. To create a qPCR test for amplifying DNA of a certain species, a species-specific primer pair and fluorescently labeled oligonucleotide probe are necessary (Kralik and Ricchi 2017). Amplification is then quantified during qPCR by measuring the intensity of fluorescence (Kralik and Ricchi 2017).

Previous efforts to develop a species-specific diagnostic assay led to the creation of molecular markers targeting unique regions in the genome of *X. necrophora* using the program RUCS (Squiers 2021). Rapid identification of PCR primers for Unique Core Sequences (RUCS),

is a program that uses whole-genome assemblies for developing unique PCR primer pairs and probes for target species (Thomsen et al. 2017). Five RUCS primer pairs specific to *X. necrophora* were designed using the best available genome of *X. necrophora* (Sharma et al. 2018) and comparing it to genomes of closely related species in the *X. arbuscula* species complex and distantly related species in the family *Xylariaceae* (Hsieh et al. 2010; U'Ren et al. 2016). Three of these RUCS-designed primers pairs showed preliminary selective amplification of *X. necrophora* (Squiers 2021).

The main goals of our study were to validate the RUCS primer pairs displaying preliminary species-specific amplification of *X. necrophora* designed by Squiers (2021), design and validate a qPCR protocol, and empirically test the newly developed qPCR assay. The outcome of our study is a sensitive, species-specific quantitative molecular assay for detecting the presence of *X. necrophora*.

MATERIALS AND METHODS

Selection of biological samples

A range of *Xylaria necrophora* (target) isolates and non-*Xylaria necrophora* (off-target) isolates from various locations (Table 1) were selected to represent species closely and distantly related to *X. necrophora* based on the phylogeny published by Garcia-Aroca et al. (2021).

2.5-year-old samples from four locations in northwestern Mississippi were stored at room temperature as fungal stroma on dried soybean debris in Falcon tubes (VWR International, Radnor, Pennsylvania) containing some of the associated soil (Table 2; Figure 1). These samples were chosen to test the assay due to their known infection status.

Soybean debris and soil samples from Winnsboro were collected from areas with low (L), moderate (M), and high (H) levels of TRD in the previous season (Table 3; Figure 2). Soil samples were collected by inserting a Falcon tube upside-down into the ground until the soil reached the 50 mL line. Soybean debris samples were collected by uprooting old soybean plants.

Growing and artificially inoculating soybean plants with Xylaria necrophora

Eight 10 cm pots of soybean plants were grown in the lab. Each pot was filled with Professional Growing Mix soil (Sungro Horticulture, Agawam, Massachusetts) with Osmocote Flower and Vegetable Smart Release® Plant Food fertilizer (ScottsMiracle-Gro, Marysville, Ohio). Each pot received five soybean seeds in a diagonal furrow across the pot. Four pots, labeled A through D, received the soybean cultivar DG 46x65 (Delta Grow Seed Co., Inc., England, Arkansas) and the other four pots, labeled E thru H, received the soybean cultivar AG4632 (Asgrow Seed Co LLC, Creve Coeur, Missouri). The pots were infected with approximately 1 teaspoon of Japanese millet inoculated with *X. necrophora* isolate DMCC2126 (Table 1) (Purvis 2019). The seeds were then covered in soil and watered. The plants were grown under supplemental lighting (Welthink LED, Hangzhou, China) and watered as needed. After 14 days, one plant per pot exhibiting the most chlorosis was extracted and photographed using a Nikon camera (Nikon, Minato City, Tokyo, Japan) with a Nikon AF-P DX 18-55mm 1:3.5-5.6G VR camera lens (Nikon, Minato City, Tokyo, Japan) on auto-flash (Figure 3).

DNA extractions

For the validation of RUCS primer pairs designed by Squiers (2021), target and off-target isolates (Table 1) were revived from 20% glycerol stocks stored at -80°C, plated on DIFCO™

potato dextrose agar (PDA) (BD, Franklin Lakes, New Jersey), and incubated at room temperature for approximately two weeks. DNA was extracted from the isolates using a modified protocol that utilizes a cetyltrimethylammonium bromide (CTAB) buffer (Doyle & Doyle, 1987; Garcia-Aroca et al. 2021). The isolates were prepared for DNA extraction by filling 1.5 mL Eppendorf (Eppendorf, New York, New York) safe-lock tubes with 1 gram of 2.0 mm zirconium beads, 1 gram of 0.5 mm beads, and 400 µL of CTAB buffer. Fungal tissue was scraped from the plates using a sterile spatula then transferred into the Eppendorf safe tubes until the tissue was submerged in buffer, with the top of the fungal tissue and buffer in line. A bullet blender (Next Advance, New York, New York) was used to grind the tissue samples for 3 minutes at 7000 rpm.

For building a qPCR standard curve, target isolates DMCC2165 (pathogenic *X. necrophora* ex-type; LA; 2017) and DMCC3828 (saprophytic *X. necrophora;* Martinique; 2005) (Garcia-Aroca et al. 2021) (Table 1) were prepared for DNA extraction using the same method for the target and off-target isolates previously described, with the exception of using Buffer AP1 (Qiagen, Hilden, Germany) instead of the CTAB buffer. DNA was extracted using a DNeasy® Plant Mini Kit (Qiagen, Hilden, Germany) following the manufacturer's protocol.

For testing the qPCR protocol on dried fungal, soybean debris, and soil samples collected in 2019 from northwestern Mississippi (Table 2; Figure 1), DNA was extracted using the modified CTAB buffer protocol (Doyle & Doyle, 1987; Garcia-Aroca et al. 2021) and DNA extraction kits. Tissue from fungal samples, consisting of stroma, were used directly in DNA extractions. Plant samples were prepared for DNA extraction by shaving the outside of the soybean tissue with a sterilized scalpel, then grinding the tissue into powder using sandpaper. DNA was extracted from the 2.5-year-old soil samples using a DNeasy® Powersoil Pro Kit (Qiagen, Hilden, Germany) following the manufacturer's protocol.

For testing the qPCR protocol on recently obtained soybean debris samples from Winnsboro, Louisiana (Table 3; Figure 2), DNA was extracted with a DNeasy® Plant Mini Kit (Qiagen, Hilden, Germany) following the manufacturer's protocol. Soybean tissue was prepared for DNA extraction following the same procedure as the 2.5-year-old plant samples. DNA was extracted from the soil samples from Winnsboro, Louisiana with a DNeasy® Powersoil Pro Kit (Qiagen, Hilden, Germany).

For testing the qPCR protocol on artificially inoculated soybean and soil samples, DNA was extracted from plant and soil samples from lab-inoculated soybean plants (Figure 3). Soybean plant samples for DNA extraction were taken from the end of the green part of the stem to the beginning of the first root. Soil samples from any soil still clumped on the roots after pulling up the selected inoculated soybean plant were used for DNA extraction. DNA was extracted from the lab-inoculated soybean plants with a DNeasy® Plant Pro Kit (Qiagen, Hilden, Germany) following the manufacturer's protocol. DNA was extracted from the soil associated with the lab-inoculated soybean plants with a DNeasy® Powersoil Pro Kit (Qiagen, Hilden, Germany) following the manufacturer's protocol.

The purity of all the extracted DNA was estimated with a Nanodrop™ Spectrophotometer (Thermo Fisher Scientific, Waltham, Massachusetts) following the manufacturer's protocol. The concentrations of the DNA were estimated with a Qubit™ dsDNA BR (broad-range) Assay Kit (Thermo Fisher Scientific, Waltham, Massachusetts) following the manufacturer's protocol. If the DNA concentrations were too low to be estimated with a Qubit™ dsDNA BR Assay Kit, a Qubit™ dsDNA HS (high-sensitivity) Assay Kit from the same manufacturer was used instead, following the manufacturer's protocol.

Validating RUCS species-specific primer pairs

Gradient PCRs for RUCS primer pairs (PP) 3 and 4 (Table 4) from Squiers (2021) were re-run in the current study to confirm *X. necrophora*-specific amplification. Gradient PCRs were run with eight different annealing temperatures from 58°C to 65°C using an MJ Mini Bio-Rad thermal cycler (Bio-Rad Laboratories, Hercules, California) with the following program: (1) 95°C for 5 minutes, (2) 95°C for 30 seconds, (3) the annealing temperature for 30 seconds, (4) 72°C for 45 seconds, (5) Repeat 2-4 thirty-four times for a total of 35 cycles, (6) a final holding temperature of 10°C (Table 5). Amplicons were visualized under UV light in a 1.5% agarose gel subjected to gel electrophoresis (60 V for 90 min) and staining with 0.01% ethidium bromide for 30 minutes.

Subsequent PCRs were run at the lowest, highest, and median annealing temperatures at which both RUCS PP3 and PP4 showed measurable amplification in the gradient PCRs (Table 5). These subsequent PCRs consisted of all five RUCS primer pairs at 58°C, and with RUCS primer pairs 2, 3, and 4 at 60°C and 62°C (Table 6).

Validating a qPCR assay for specific detection of Xylaria necrophora

The corresponding qPCR probe for RUCS PP3 was selected for our assay based on the results from our validation of the RUCS species-specific primer pairs (Table 4; Table 5). The probe was a 100 nm PrimeTime® qPCR with HPLC purification from IDT (Integrated DNA Technologies, Inc, Coralville, Iowa) with two fluorescent dyes: 6-FAM for the 5’ end and TAMRA for the 3’ end (Table 4).

One 96-well skirted plate (Bio-Rad Laboratories, Hercules, California), one 10 mL Falcon tube (VWR International, Radnor, Pennsylvania), three 0.2 mL 8-Well PCR strip tubes (Neptune

Scientific, Toronto, Ontario), and three 0.6 mL tubes were treated with ultraviolet light in an UV Crosslinker (VWR International, Radnor, Pennsylvania) for 20 minutes.

Forward and reverse primers, the qPCR probe, iTaq Universal Probes Supermix (Bio-Rad Laboratories, Hercules, California), and extracted DNA from isolates DMCC2165 and DMCC3828 (Table 1) were kept on ice throughout plate setup. To avoid degradation due to fluorescent light exposure, the qPCR probe container was wrapped in aluminum foil. Eight serial dilutions of DNA extracted from isolates DMCC2165 and DMCC3828 were made in two of the strip tubes by standardizing the DNA of an isolate to 20 ng/ μL in the first tube, then diluting 4 μL of the mixture into 16 μL of nuclease-free water (NFW) in the subsequent tube. The process was repeated for the remaining dilutions. 10 μL of NFW was pipetted into each tube of the third strip tube. The RUCS PP3 forward and reverse primers, diluted at 10 mM from stocks, and their corresponding qPCR probe (Table 4), were diluted 1:10 using NFW in 0.6 mL tubes.

To make a qPCR reaction pre-mix, the following amounts of each component were pipetted into the 10 mL Falcon tube: 890 μL NFW, 1250 μL iTaq Universal Probes Supermix, 100 μL each of the RUCS PP3 forward and reverse primer dilutions, and 60 μL of the RUCS PP3 qPCR probe dilution. To set up the reaction plate, 24 μL of the qPCR pre-mix was distributed into each well of the 96-well skirted plate using a multichannel pipette. DNA was loaded into the plate by using a multichannel pipette to distribute 1 μL from each well of the DMCC2165 serial dilutions strip tube into columns 1-4 and 1 μL from each well of the DMCC3828 serial dilutions strip tube into columns 5-8. Using the multichannel pipette, 1 μL of NFW was pipetted into each well of columns 9 and 10 for the negative controls, and columns 11 and 12 were left with only pre-mix for the non-template controls (NTC). The plate was sealed with Microseal ‘B’ seal plate film (Bio-Rad Laboratories, Hercules, California), spun for 30 seconds in a Centrifuge 5810 R (Eppendorf,

Hamburg, Germany), then placed in a CFX96-Connect Thermocycler (Bio-Rad Laboratories, Hercules, California) and run with a user-defined protocol by following the manufacturer's instructions.

CFX Manager™ Software (Bio-Rad Laboratories, Hercules, California) was used to create a user-defined protocol and plate. Our user-defined protocol was designed with the following steps: (1) 95.0°C for 5 minutes, (2) 95.0°C for 30 seconds, (3) 56.0°C for 20 seconds, (4) 72.0°C for 45 seconds, (5) Plate Read, (6) Repeat steps 2-5 39 more times for a total of 40 cycles. The cycle threshold was automatically determined by CFX Manager™ Software.

The qPCR protocol was repeated using the DNA extracted from the off-target isolates (Table 1). The off-target DNA and the target DNA from DMCC2165 and DMCC3828, chosen as the positive controls, was standardized to a concentration of 4 ng/µL.

qPCR of field-obtained fungal, soybean, and soil samples collected in 2019

DNA extracted from the 2.5-year-old fungal, soybean, and soil samples was standardized to a concentration of 4 ng/µL (Table 2; Figure 1). qPCR was run with these DNA samples according to our protocol.

qPCR of field-obtained soybean and soil samples collected in 2022

DNA extracted from the soybean plant debris and soil samples from Winnsboro (Table 3; Figure 2) was standardized to a concentration of 4 ng/µL. qPCR was run with this DNA according to our protocol. qPCR was repeated according to our protocol with DNA from a selection of the soil samples—1-S, 2-S, 3-S, 4-S, 5-S, 6-S, 7-S, 8-S, 11-S, 12-S, 13-S, 20-S—that had not been standardized.

qPCR of lab-inoculated soybean and soil samples

DNA extracted from soybean tissue and associated soil samples from the lab-inoculated plants (Figure 3) was used to run qPCR following our protocol.

Data analysis

Excel (Microsoft, Redmond, Washington) was used to build a standard curve equation to determine the correlation between *X. necrophora* DNA concentration and cycle threshold from relative fluorescence units (RFUs) detected in qPCR. The concentration of eight serial dilutions of two *X. necrophora* isolates, DMCC2165 and DMCC3828, were converted from ng/µL to ng/L to calculate logarithmic DNA concentrations. The mean cycle threshold per dilution was calculated and a linear model for mean cycle threshold by log DNA concentration of the qPCR results (Figure 4) was graphed. The graph provides the standard curve equation and its respective linear correlation coefficient (R^2).

Google Earth (Google, Mountain View, California) was used to display geographic locations of old samples from northwestern Mississippi (Figure 1) and recent samples from Winnsboro, Louisiana (Figure 2).

RESULTS

Validating RUCS species-specific primer pairs

Gradient PCR of RUCS primer pair 3 showed visible amplification of target DMCC2470 at 58°C, 59°C, 60°C, 61°C, 62°C, and 64°C (Table 5). Gradient PCR of RUCS primer pair 4 showed visible amplification of target DMCC2470 at 58°C, 59°C, 60°C, 61°C, 62°C, 63°C, and 65°C and of the off-target DMCC3361 at 58°C, 59°C, 60°C, 61°C, 63°C, and 65°C.

PCRs of the five RUCS primer pairs (PP) at 58°C resulted in both target and off-target amplification (Table 6). PP1 showed visible amplification of all targets as well as seven off-target. PP2 showed visible amplification of four out of five targets as well as six off-targets. PP3 showed visible amplification of all targets as well as five off-targets. PP4 showed visible amplification of four out of five targets as well as six off-targets. PP5 showed visible amplification of all targets as well as thirteen off-targets.

PCRs of RUCS PP2, PP3, and PP4 at 60°C resulted in both target and off-target amplification (Table 6). PP2 showed visible amplification of all targets as well as four off-targets. PP3 showed visible amplification of five out of six targets as well as two off-targets. PP4 showed visible amplification of all targets as well as three off-targets.

PCRs of RUCS PP2, PP3, and PP4 at 62°C resulted in both target and off-target amplification (Table 6). PP2 showed visible amplification of all targets as well as four off-targets. PP3 showed visible amplification of two out of six targets as well as seven off-targets. PP4 showed visible amplification of all targets as well as two off-targets.

For all PCRs, amplification of off-targets consisted of fainter bands compared to targets, as viewed under UV light on ethidium bromide-stained gel.

Validating a qPCR assay for specific detection of Xylaria necrophora

The relative fluorescence units (RFU) per cycle observed using a log scale showed measurable, concentration-dependent amplification of all four technical replicates of all eight serial dilutions of both targets DMCC2165 and DMCC3828 (Figure 4). The mean cycle threshold at which each target DNA concentration amplified were: 17.7 for 20 ng/µL, 20.0 at for 4 ng/µL,

22.9 for 0.8 ng/µL, 25.1 for 0.16 ng/µL, 27.6 for 0.032 ng/µL, 30.1 for 0.0064 ng/µL, 32.6 for 0.00128 ng/µL, and 36.0 for 0.000256 ng/µL.

The standard curve equation was calculated to be $y = -3.5337x + 43.353$ ($R^2 = 0.9993$), where x = log DNA concentration (ng/L) and y = cycle threshold (Figure 5). Using this equation, the limit of detection for 40 cycles of qPCR was 0.000001 ng of target DNA.

For the qPCR using off-target DNAs, the RFU per cycle observed using a log scale showed the positive controls DMCC2165 and DMCC3828 had measurable amplification at a mean cycle threshold of 22.5 (Figure 6). The mean cycle threshold at which off-targets showed measurable amplification were: 35.5 for DMCC3361, 36.5 for DMCC4044, and 36.7 for DMCC4042. The cycle threshold at which off-targets with one technical replicate that showed measurable amplification were: 39.7 for DMCC3822 and 37.8 for DMCC3830. Off-targets without measurable amplification included: DMCC2087, DMCC2966, DMCC3307, DMCC3465, DMCC3823, DMCC4041, DMCC4045, DMCC3879, and DMCC4043.

qPCR of field-obtained fungal, soybean, and soil samples collected in 2019

The RFU per cycle observed using a log scale showed the positive controls DMCC2165 and DMCC3828 had measurable amplification at a mean cycle threshold of 16.3 (Figure 7). The mean cycle thresholds at which samples showed measurable amplification were: 30.8 for Bolivar-P, 23.0 for Bolivar-S, 24.8 for Clarksdale-F, 28.5 for DeSoto-S, 20.1 for TA090519-F, 19.13 for TA090519-P, and 24.9 for TA090519-S. One technical replicate of DeSoto-P showed measurable amplification at a cycle threshold of 22.6. The samples without measurable amplification included: Bolivar-F, Clarksdale-P, and Clarksdale-S.

qPCR of field-obtained soybean and soil samples collected in 2022

The RFU per cycle observed using a log scale showed the positive controls DMCC2165 and DMCC3828 had measurable amplification at a mean cycle threshold of 18.5 (Figure 8). All three technical replicates of the sample 1-P showed measurable amplification at a mean cycle threshold of 24.4. One of the three technical replicates of the negative control showed measurable amplification at a cycle threshold of 38.27. Sample 2-P did not show any measurable amplification. None of the soil samples, standardized to 20 ng/µL, showed any measurable amplification.

Upon repeating qPCR with a selection of the field-obtained soil samples collected in 2022 that had not been standardized to 20 ng/µL, there were samples with measurable amplification (Figure 9). The positive controls DMCC2165 and DMCC3828 showed measurable amplification at a mean cycle threshold of 15.6. The cycle thresholds at which measurable amplification occurred for one technical replicate of a sample were: 5.2 for 2-S, 37.4 for 3-S, 37.1 for 5-S, 36.2 for 7-S, and 36.3 for 20-S. Two technical replicates of 13-S showed measurable amplification at a mean cycle threshold of 37.2. Two technical replicates of the negative control showed measurable amplification at cycle thresholds 5.5 and 35.6. One technical replicate of the non-template control showed measurable amplification at a cycle threshold of 35.6. Sample 2-S and one technical replicate of the negative control exhibited a unique amplification pattern, beginning with measurable amplification at cycles 5.2 and 5.5, respectively, and maintaining a weaker slope of amplification as compared to the other samples. The samples without any measurable amplification included: 1-S, 4-S, 6-S, 8-S, 11-S, and 12-S.

qPCR of lab-inoculated soybean and soil samples

Plants A and E exhibited more visible chlorosis than the other plants (Figure 3). Plants C and H exhibited barely, if any, visible chlorosis. The positive controls had measurable amplification at a mean cycle threshold of 15.6 (Figure 10). The cycle thresholds at which measurable amplification occurred for one technical replicate of a sample were: 36.0 for A-P, 36.2 for B-P, 35.9 for D-P, 36.1 for F-P, 35.9 for G-P, 35.9 for C-S, 38.3 for D-S, and 36.5 for E-S. Three technical replicates of B-S showed measurable amplification, one at a cycle threshold of 4.11 and the other two at a mean cycle threshold of 37.1. Two technical replicates of the negative control showed measurable amplification at cycle thresholds 5.5 and 35.6. One technical replicate of the non-template control showed measurable amplification at a cycle threshold of 35.6. One technical replicate of B-S and the negative control exhibited a unique amplification pattern, beginning with measurable amplification at cycles 4.11 and 5.5, respectively, and maintaining a weaker slope of amplification as compared to other samples. The samples without any measurable amplification included: C-P, E-P, H-P, A-S, F-S, G-S, and H-S.

DISCUSSION

Xylaria necrophora is an emerging pathogen of soybean in the southern United States that has the potential to cause significant crop yield losses (Allen et al. 2017, 2018, 2019, 2020). Current detection of this pathogen mostly relies on recognition of the symptoms associated with TRD (Allen et al. 2017). The pathogen can be isolated from plants diagnosed with TRD, but the process of confirming the presence and identity of the pathogen can be lengthy (Allen et al. 2017; Squiers 2021). Early and rapid detection of plant pathogens in agricultural systems is challenging, but new technologies and sensitive tests targeting specific genomic regions of pathogens can

provide reliable approaches for diagnostic purposes, including soybean pathogens (Chanda et al. 2014). In our study, we have determined the best parameters to detect the DNA of *X. necrophora* using qPCR. We validated our results using known strains of the pathogen by determining the optimum parameters to consistently detect its DNA at different concentrations and building a standard curve. We further validated our assay by amplifying DNA of the pathogen present in field-obtained fungal, plant, and soil samples and in lab-inoculated plant and soil samples.

RUCS primer pairs 3 and 4 were chosen to run gradient PCR due to their preliminary selective amplification of *X. necrophora* (Squiers 2021). Both RUCS primer pairs 3 and 4 showed measurable amplification of *X. necrophora* isolate DMCC2470 from an annealing temperature range of 58°C to 62°C (Table 5). In the subsequent PCRs, annealing temperature was set to one of the two extremes (58°C and 62°C) or the median temperature (60°C) (Table 6). Since RUCS primer pair 3 with an annealing temperature of 60°C had the least off-target amplification of any other primer pair and annealing temperature combination (Table 6), this primer pair, probe, and annealing temperature combination was chosen to run qPCR. However, the first qPCR with an annealing temperature of 60°C showed no clear amplification, so we lowered the annealing temperature to 56°C.

RUCS primer pair 3 off-target amplicons were very faint on the agarose gels stained with ethidium bromide and viewed under UV light, and appeared of smaller size than the amplicons of *X. necrophora*. These results were confirmed in subsequent qPCR assays because amplification of off-target DNA was observed only after 35 cycles (Figure 6). The intensity difference in the PCR bands of off-target and target DNA samples suggests amplification may have been due to primer-dimer rather than amplification of the off-target DNA (Brownie et al. 1997).

Validation of the qPCR protocol using serial dilutions of *X. necrophora* DNA showed concentration-dependent amplification. Target DNA diluted to 0.000256 ng/µL was consistently detected at 36 cycles (Figure 4). During this qPCR, only one of the sixteen negative controls showed measurable amplification (Figure 4), indicating one well was contaminated with *X. necrophora* DNA during plate set-up or a false positive. The measurable amplification of the technical replicate of DMCC2165 diluted to 20 ng/µL from cycles 1 to 4 (Figure 4) may have also been a false positive or been due to primer dimer (Brownie et al. 1997). The standard curve equation calculated from this qPCR demonstrates a strong correlation between log DNA concentration (ng/L) and cycle threshold ($R^2 = 0.9993$, Figure 5) with a negative slope, suggesting an increase in the template DNA concentration will require less PCR cycles to reach the amplification threshold.

The qPCR assay detected *X. necrophora* DNA in field-obtained 2.5-year-old fungal, infected plant, and associated soil samples (Figure 7). DNA from these samples was expected to be somewhat degraded, but detection of the target DNA was possible with our assay. These results suggest this qPCR assay can be used in samples collected in the previous season to confirm the presence of the pathogen in specific areas where it is suspected.

The qPCR assay detected *X. necrophora* DNA in one of two field-obtained infected plant samples from an area of moderate TRD levels (Figure 8). However, this does not necessarily mean only one of the two soybean plants were infected; *X. necrophora* may have been able to be isolated from only certain parts of the plant. In the future, testing various parts of the soybean plant may provide insight as to where *X. necrophora* is most likely to be detected in soybean. The qPCR assay did not initially detect *X. necrophora* DNA in the field-obtained soil samples standardized to 20 ng/µL from areas of low, moderate, and high TRD levels. However, repeating the qPCR with

a selection of those soil samples that had not been standardized demonstrated different results: some soil samples showed measurable amplification, but only after 36 cycles (Figure 9). These results may indicate that a higher amount of target DNA is necessary for detection by our assay.

The qPCR assay detected *X. necrophora* DNA in the lab-inoculated plant and associated soil samples (Figure 10). However, only one sample had all of its technical replicates showing measurable amplification, and almost all the samples that amplified did so after cycle 35 (Figure 10). Additionally, one soil sample from the lab-inoculated plant exhibited a unique amplification pattern, where amplification was first measured at cycle 4 and maintained a weak slope for the remainder of qPCR. This was also seen in one technical replicate of a soil sample from the field with high TRD levels and in one technical replicate of the negative control (Figure 9; Figure 10). This unique amplification pattern may suggest the presence of some sample-specific PCR inhibition, but not enough to yield a negative result (Brunstein 2015). If sample-specific PCR inhibition occurs widely throughout our samples, this potentially explains the incidences where our qPCR assay does not amplify DNA extracted from samples known to be infected with or be in close proximity to *X. necrophora*.

The qPCR protocol developed in our study has demonstrated sensitive, species-specific amplification of *X. necrophora* in fungal, soybean plant, and soil samples. As TRD continues to impact soybean, and potentially other crops in the southern United States, this qPCR protocol may provide rapid confirmation of suspected TRD cases and thus aid with the mitigation process. Furthermore, because of its sensitivity, this assay can be used to document the distribution of *X. necrophora* in agricultural and non-agricultural systems across the United States and, potentially, the global distribution of this significant pathogen.

ACKNOWLEDGEMENTS

We thank Jonathan Richards, Jeremy Brown, Teddy Garcia-Aroca, and Vinson Doyle for serving on the thesis committee. We thank everyone at the Doyle Mycology Lab, especially Ernesto da Silva for growing infected soybean plants, Aaron DeVries for helping extract DNA from soil samples, and Elaisa Tubana for organizing and finding access to materials. We thank Tom Allen from Mississippi State University for collecting many of the specimens used in our study. We thank Trey Price for assisting with sample collection in Winnsboro, Louisiana. We also thank the Department of Plant Pathology and Crop Physiology at Louisiana State University.

REFERENCES

Allen, T., Bluhm, B., Conner, K., Doyle, V., Price, T., Sikora, E., Singh, R., Spurlock, T., Tomaso-Peterson, M., & Wilkerson, T. (2017). First Description of the Causal Agent of Taproot Decline of Soybean, an Emerging Disease in the Southern United States. *Plant Health Progress, 18*(1), 35–40. https://doi.org/10.1094/PHP-01-17-0004-RS

Allen TW, Bissonnette K, Bradley CA, Damicone JP, Dufault NS, Faske TR, Hollier CA, Isakeit T, Kemerait RC, Kleczewski NM, Mehl HL, Mueller D. J, Overstreet C, Price PP, Sikora EJ, Spurlock TN, Thiessen L, Young H. 2018. Southern United States soybean disease yield loss esti- mates for 2017. Proceedings of the 45th Annual Meeting of the Southern Soybean Disease Workers; Pensacola Beach, Florida; 7–8 March 2018; Southern Soybean Disease Workers (SSDW). p. 31–39.

Allen TW, Bissonnette K, Bradley CA, Damicone JP, Dufault NS, Faske TR, Hollier CA, Isakeit T, Kemerait RC, Kleczewski NM, Mehl HL, Mueller D. J, Overstreet C, Price PP, Sikora EJ, Spurlock TN, Thiessen L, Young H. 2019. Southern United States soybean disease yield loss esti- mates for 2018. Proceedings of the 46th Annual Meeting of the Southern Soybean Disease Workers; Pensacola Beach, Florida; 6–7 March 2019; Southern Soybean Disease Workers (SSDW). p. 28–36.

Allen TW, Bissonnette K, Bradley CA, Damicone JP, Dufault NS, Faske TR, Isakeit T, Kemerait RC, Koehler A, Mehl HL, Muller JD, Padgett GB, Price PP, Sikora EJ, Small IM, Thiessen L, Young H. 2020. Southern United States soybean disease loss estimates for 2019. Southern Soybean Disease Workers (SSDW). p. 1–10. Available online at https://www.mssoy.org/uploads/files/allen-dis- loss-survey-2019.pdf

Aoki T, O'Donnell K, Scandiani MM. 2005. Sudden death syndrome of soybean in South America is caused by four species of Fusarium: Fusarium brasiliense sp. nov., F. cuneirostrum sp. nov., F. tucumaniae, and F. virguliforme. *Mycoscience*. 46:162–183.

Boesenberg-Smith, K. A., Pessarakli, M. M., & Wolk, D. M. (2012). Assessment of DNA Yield and Purity: An Overlooked Detail of PCR Troubleshooting. *Clinical Microbiology Newsletter*, *34*(1), 1–6. https://doi.org/10.1016/j.clinmicnews.2011.12.002

Brownie, J., Shawcross, S., Theaker, J., Whitcombe, D., Ferrie, R., Newton, C., & Little, S. (1997). The elimination of primer-dimer accumulation in PCR. *Nucleic Acids Research*, *25*(16), 3235. https://doi.org/10.1093/nar/25.16.3235

Brunstein, J. (2015). Interpretation of qPCR curve shapes. *Medical Laboratory Observer*. https://www.mlo-online.com/home/article/13008268/interpretation-of-qpcr-curve-shapes

Chanda, A. K., Ward, N. A., Robertson, C. L., Chen, Z.-Y., and Schneider, R. W. 2014. Development of a quantitative polymerase chain reaction detection prot ocol for Cercospora kikuchii in soybean leaves and its use for documenting latent in fection as affected by fungicide applications. Phytopathology 104:1118-1124.

Chang H-X, Radwan O, Hartman GL, Domier LL, Hudson ME, Yendrek CR. 2015. Identification of multiple phytotoxins produced by *Fusarium virguliforme* including a phytotoxic effector (FvNIS1) associated with sudden death syndrome foliar symptoms. Molecular Plant-Microbe Interactions. 29:96–108.

Doyle JJ, Doyle JL. 1987. A rapid DNA isolation procedure for small quantities of fresh leaf tissue. Phytochemical Bulletin 19:11–15.

Garcia-Aroca, T., Price, P. P., Tomaso-Peterson, M., Allen, T. W., Wilkerson, T. H., Spurlock, T. N., Faske, T. R., Bluhm, B., Conner, K., Sikora, E., Guyer, R., Kelly, H., Squiers, B. M.,

& Doyle, V. P. (2021). Xylaria necrophora, sp. Nov., is an emerging root-associated pathogen responsible for taproot decline of soybean in the southern United States. *Mycologia*, *113*(2), 326–347. https://doi.org/10.1080/00275514.2020.1846965

Hartman GL, Huang YH, Li S. 2004. Phytotoxicity of Fusarium solani culture filtrates from soybeans and other hosts assayed by stem cuttings. Australasian Plant Pathology. 33:9–15.

Higuchi, R., Fockler, C., Dollinger, G., and Watson, R., Kinetic PCR analysis: real-time monitoring of DNA amplification reactions. *Biotechnology*, 11(9): 1026-1030, 1993

Hsieh HM, Lin CR, Fang MJ, Rogers JD, Fournier J, Lechat C, Ju YM. 2010. Phylogenetic status of Xylaria subgenus Pseudoxylaria among taxa of the subfamily Xylarioideae (Xylariaceae) and phylogeny of the taxa involved in the subfamily. Molecular Phylogenetics and Evolution 54:957–969.

Kralik, P., & Ricchi, M. 2017. A Basic Guide to Real Time PCR in Microbial Diagnostics: Definitions, Parameters, and Everything. *Frontiers in Microbiology*, *8*. https://www.frontiersin.org/article/10.3389/fmicb.2017.00108

O'Donnell K, Moustafa AF, Aoki T, Brankovics B, Cano-Lira JF, Coleman JJ, Hoog GS de, Pietro A Di, Frandsen RJN, Geiser DM, Gibas CFC, Guarro J, Kim H, Kistler HC, Laraba I, Leslie JF, López-berges MS, Lysøe E, Meis JF, Monod M, Proctor RH, Rep M, Wingfield MJ, Zhang N, Zhang X. 2020. No to Neocosmospora: Phylogenomic and practical reasons for continued inclusion of the *Fusarium solani* species complex in the genus *Fusarium*. *Mycosphere*. 5:1–7.

Purvis, M. (2019). *Developing Management Strategies for Taproot Decline, Xylaria sp., in Soybean* [Master's Thesis]. Louisiana State University.

Sharma S, Zaccaron AZ, Ridenour JB, Allen TW, Conner K, Doyle VP, Price T, Sikora E, Singh R, Spurlock T, Tomaso-peterson M, Wilkerson T, Bluhm BH. 2018. Draft genome sequence of Xylaria sp., the causal agent of taproot decline of soybean in the southern United States. Data in Brief. 17:129–133.

Squiers, B. M. (2021). *Designing and Evaluating the Utility of Novel Primers for the Detection of an Emerging Fungal Disease of Soybean* [Undergraduate Honors Thesis]. Louisiana State University.

Thomsen, M. C. F., Hasman, H., Westh, H., Kaya, H., & Lund, O. (2017). RUCS: Rapid identification of PCR primers for unique core sequences. *Bioinformatics (Oxford, England)*, *33*(24), 3917–3921. https://doi.org/10.1093/bioinformatics/btx526

U'Ren JM, Miadlikowska J, Zimmerman NB, Lutzoni F, Stajich JE, Arnold AE. 2016. Contributions of North American endophytes to the phylogeny, ecology, and taxonomy of Xylariaceae (Sordariomycetes, Ascomycota). Molecular Phylogenetics and Evolution 98:210–232.

TABLES AND FIGURES

Table 1. Isolates and their geographical origin as described in the Doyle Mycology Culture Collection (DMCC). These isolates represent a variety of species both distantly and closely related to *X. necrophora*, as seen in the phylogeny presented by Garcia-Aroca (2021). Isolates of the species *Xylaria necrophora* are also referred to as "target" samples throughout our study, and isolates that are not of the species *X. necrophora* are referred to as "off-target" samples.

Isolate (DMCC)	Species	Origin
2087	*Curvularia lunata*	LA
2966	*Colletotrichum siamense*	LA
3307	*Nemania primolutea*	LA
3465	*Xylaria cubensis*	GA
3822	*Xylaria allantoidea*	OH
3823	*Xylaria polymorpha*	OH
3361	*Xylaria multiplex*	LA
3830	*Xylaria cf. venustula*	LA
4044	*Xylaria bambusicola*	Thailand
4041	*Xylaria arbuscula var. plenofissura*	Taiwan
4045	*Xylaria venosula*	USA
4042	*Xylaria arbuscula*	Taiwan
3879	*Xylaria arbuscula*	LA
4043	*Xylaria striata*	China
3828	*Xylaria necrophora*	Martinique
2622	*Xylaria necrophora*	AL
2119	*Xylaria necrophora*	MS
2470	*Xylaria necrophora*	AR
2165	*Xylaria necrophora*	LA
2126	*Xylaria necrophora*	LA

Table 2. Geographic coordinates and counties of the four locations where fungal, plant, and soil samples were collected in northwestern Mississippi in 2019 (Figure 1).

Sample	County	Latitude	Longitude
Bolivar	Bolivar	34° 49' 0.3972"N	89° 54' 21.7368"W
Clarksdale	Clarksdale	34° 10' 36.8472"N	90° 36' 3.9528"W
DeSoto	DeSoto	33° 50' 8.7638"N	90° 50' 53.0873"W
TA090519	Sunflower	33° 32' 22.1712"N	90° 45' 16.2684"W

Table 3. Geographic locations of soil (S) and soybean plant (P) samples collected in Winnsboro, Louisiana in 2022 (Figure 2). Samples were taken from areas of low (L), moderate (M), and high (H) levels of TRD (Trey Price, personal communication).

Sample	TRD Level	Latitude	Longitude
1-S	M	32°08'19.5"N	91°42'07.2"W
2-S	M	32°08'20.3"N	91°42'06.8"W
3-S	M	32°08'20.7"N	91°42'06.1"W
4-S	M	32°08'22.3"N	91°42'05.5"W
5-S	M	32°08'22.5"N	91°42'05.4"W
6-S	H	32°08'19.9"N	91°41'59.3"W
7-S	H	32°08'20.7"N	91°41'59.9"W
8-S	H	32°08'21.2"N	91°41'59.0"W
9-S	H	32°08'22.5"N	91°41'58.4"W
10-S	H	32°08'23.5"N	91°41'59.4"W
11-S	L	32°08'31.8"N	91°41'40.5"W
12-S	L	32°08'31.8"N	91°41'40.5"W
13-S	L	32°08'31.6"N	91°41'40.5"W
14-S	L	32°08'29.7"N	91°41'42.2"W
15-S	L	32°08'29.6"N	91°41'42.8"W
16-S	M	32°08'26.6"N	91°41'40.2"W
17-S	M	32°08'26.6"N	91°41'40.2"W
18-S	M	32°08'26.6"N	91°41'40.2"W
19-S	M	32°08'26.6"N	91°41'40.2"W
20-S	M	32°08'26.6"N	91°41'40.2"W
21-S	H	32°08'23.6"N	91°41'13.8"W
22-S	H	32°08'23.1"N	91°41'13.2"W
23-S	H	32°08'22.7"N	91°41'12.7"W
24-S	H	32°08'22.7"N	91°41'12.5"W
25-S	H	32°08'22.7"N	91°41'12.5"W
26-S	L	32°08'12.1"N	91°41'29.7"W
27-S	L	32°08'12.1"N	91°41'29.7"W
28-S	L	32°08'12.1"N	91°41'29.7"W
29-S	L	32°08'12.1"N	91°41'29.7"W
30-S	L	32°08'12.1"N	91°41'29.7"W
31-S	L	32°08'04.9"N	91°41'54.5"W
32-S	L	32°08'04.9"N	91°41'54.5"W
33-S	L	32°08'05.7"N	91°41'55.4"W
34-S	L	32°08'05.7"N	91°41'55.4"W
35-S	L	32°08'06.2"N	91°41'54.2"W
1-P	M	32°08'26.4"N	91°41'42.0"W
2-P	M	32°08'26.6"N	91°41'40.2"W

Table 4. DNA sequences of RUCS primer pairs (PP) 1, 2, 3, 4, and 5 forward and reverse primers, as designed by Squiers (2021), as well as the corresponding qPCR probe for RUCS PP3.

		Sequence
PP1	Forward primer	5’-AGCGTCATTAGTTCCAGGCAA-3’
	Reverse primer	5’-CAACGCTGTATGTCTGATGCC-3’
PP2	Forward primer	5’-CGTTAGAGTATCGCCGGTCTC-3’
	Reverse primer	5’-TGCGGTCTAGAGGCTACAGAT-3’
PP3	Forward primer	5’-AGCAGCTTACCAAATCCCCAA-3’
	Reverse primer	5’-ACGGCTATAACCTCGATGTCG-3’
	qPCR probe	5’-6-FAM-TACAAACGGGCAGGGACCAAGGCG-TAMRA-3’
PP4	Forward primer	5’-TCCGGATCCCACTTAACCTCT-3’
	Reverse primer	5’-TGTGCCTAATCTCACCGTTCC-3’
PP5	Forward primer	5’-CCTGAGCCAAAGAGATGTGGT-3’
	Reverse primer	5’-CGGTGACACTAGAAGATGGCA-3’

Table 5. Results of amplification in gradient PCRs with RUCS primer pairs (PP) 3 and 4 designed by Squiers (2021) on a range of target and off-target isolates from the Doyle Mycology Culture Collection (DMCC) (Table 1). PCR amplification was visualized under UV light in a 1.5% agarose gel subjected to gel electrophoresis (60 V for 90 min) and staining with 0.01% ethidium bromide for 30 minutes. Temperature for each primer pair denotes the annealing temperature of the PCR. A plus sign (+) denotes visible amplification of a target (*X. necrophora*) isolate, a letter x (x) denotes visible amplification of an off-target (non-*X. necrophora*) isolate, and a blank represents no visible amplification.

Isolate (DMCC)	**RUCS PP 3**								**RUCS PP 4**							
	58 °C	59°C	60 °C	61 °C	62 °C	63 °C	64 °C	65 °C	58 °C	59 °C	60 °C	61 °C	62 °C	63 °C	64 °C	65 °C
3307																
3361									x	x	x	x		x		x
4044																
4042																
2470	+	+	+	+	+		+		+	+	+	+	+	+		+
NFW																

Table 6. PCR results from five RUCS primer pairs (PP) designed by Squiers (2021) on a range of target and off-target isolates from the Doyle Mycology Culture Collection (DMCC) (Table 1). PCR amplification was visualized under UV light in a 1.5% agarose gel subjected to gel electrophoresis (60 V for 90 min) and staining with 0.01% ethidium bromide for 30 minutes. Temperature for each primer pair denotes the annealing temperature of the PCR. A plus sign (+) denotes visible amplification of a target (*X. necrophora*) isolate, a letter x (x) denotes visible amplification of an off-target (non-*X. necrophora*) isolate, and a blank represents no visible amplification. NA denotes PCR results that are not available.

Isolate	**PP1**	**PP2**			**PP3**			**PP4**			**PP5**
(DMCC)	58°C	58°C	60°C	62°C	58°C	60°C	62°C	58°C	60°C	62°C	58°C
2087							x				x
2966	x	x			x		x				x
3307											x
3465	x	x						x			x
3822								x			x
3823								x			
3361	x	x	x	x			x		x		x
3830	x	x	x	x	x				x		x
4044					x		x				x
4041											x
4045	x					x	x				x
4042	x		x			x	x	x	x		x
3879		x	x	x	x			x		x	x
4043	x	x		x	x		x	x		x	x
3828		+	+	+	+	+	+	+	+	+	+
2622	+	+	+	+	+	+		+	+	+	+
2119	NA	NA	+	+	NA		+	NA	+	+	NA
2165	+		+	+	+	+			+	+	+
2477	+	+	+	+	+	+		+	+	+	+
3464	+	+	+	+	+	+		+	+	+	+
NFW											

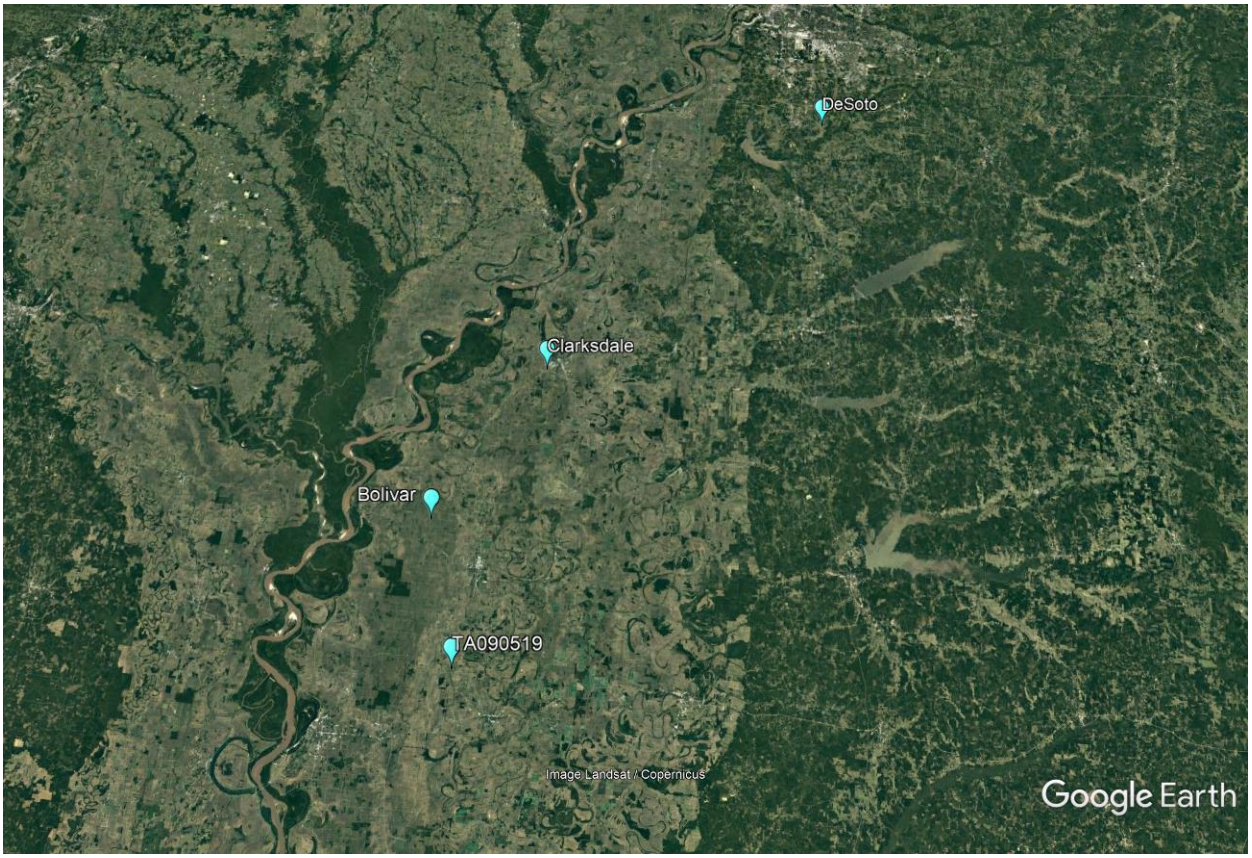

Figure 1. Map of northwestern Mississippi displaying locations of fungal, plant, and soil samples collected in 2019 (Table 2).

Figure 2. Map of field-obtained soil (S) and soybean (P) samples in Winnsboro, Louisiana (Table 3). Color pink denotes samples in areas with high levels of taproot decline of soybean (TRD), white denotes samples in areas with moderate levels of TRD, and green denotes samples in areas with low levels of TRD.

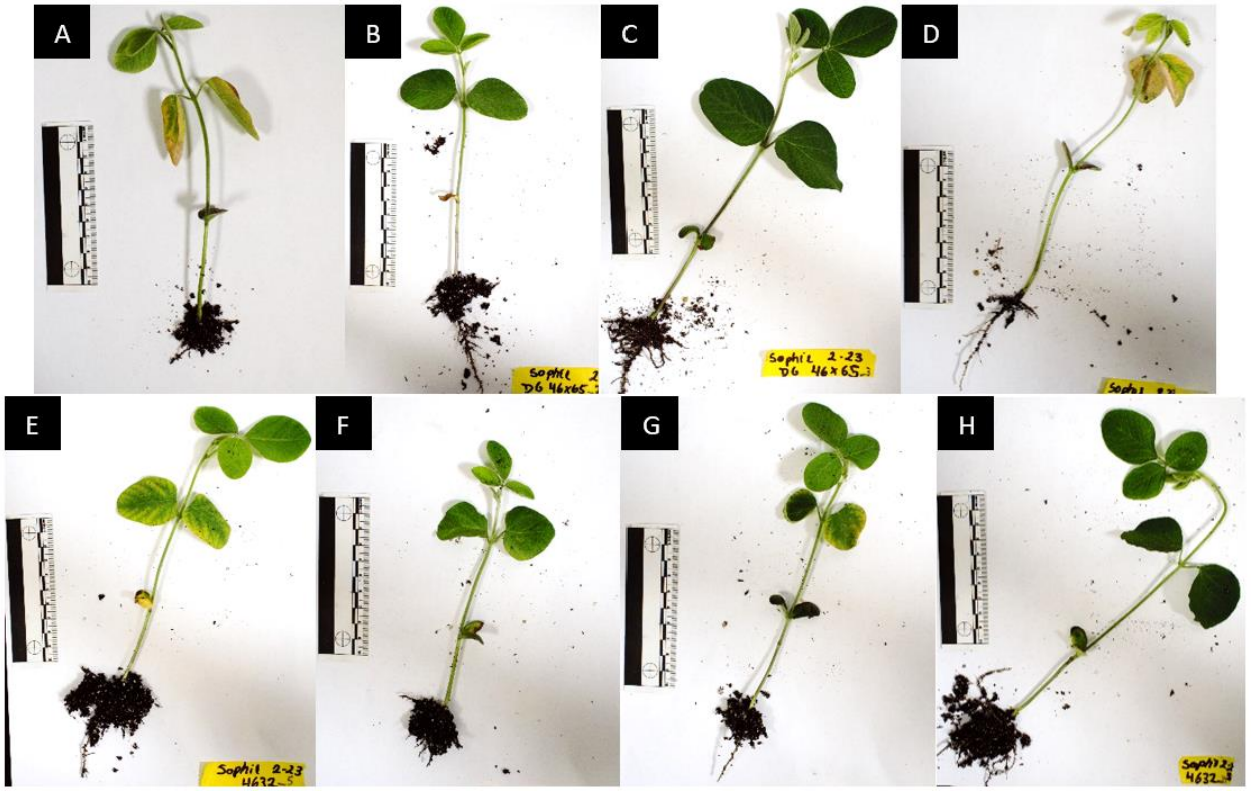

Figure 3. Photographs of soybean plants, artificially inoculated with DMCC2126, fourteen days after being planted (Table 1). Plants A through D were soybean cultivar DG 46x65 (Delta Grow Seed Co., Inc., England, Arkansas) and plants E through H were soybean cultivar AG 4632 (Asgrow Seed Co LLC, Creve Coeur, Missouri).

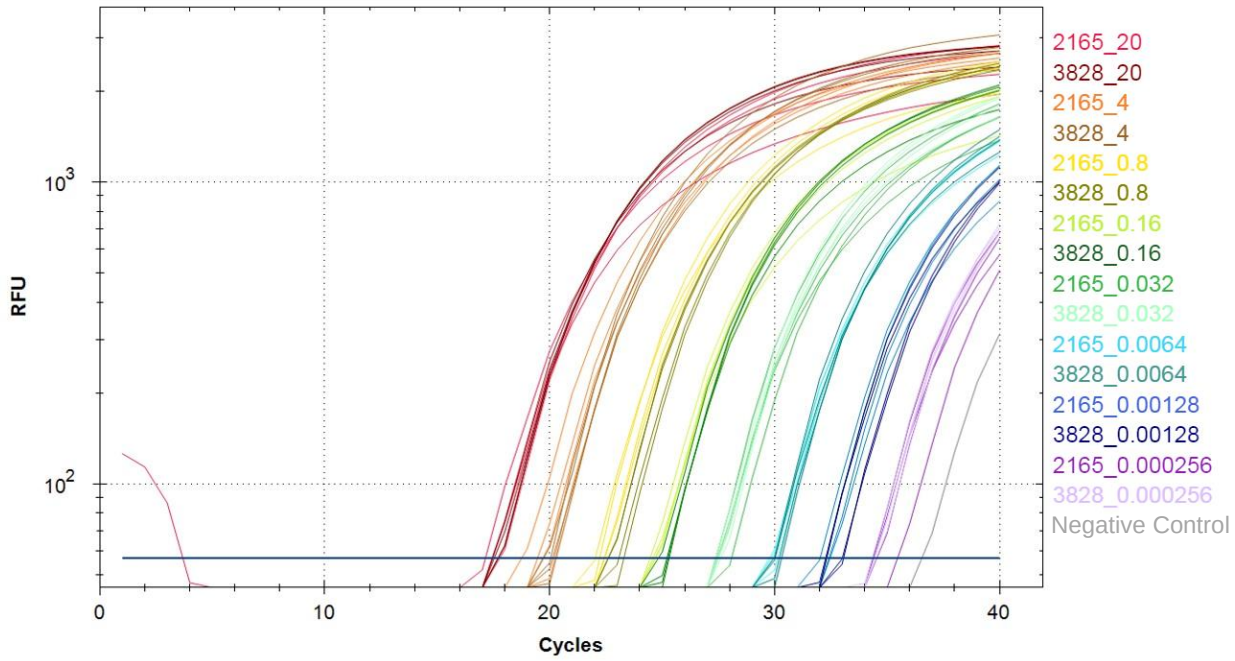

Figure 4. qPCR results from serial dilutions of *Xylaria necrophora* isolates DMCC2165 and DMCC3828 (Table 1). Results are depicted as color-coded lines representing relative fluorescence units (RFU) by number of cycles using a log scale. Each label is stylized as isolate_dilution(ng/µL) with a unique color. There are four technical replicates of each biological sample, sixteen technical replicates of the negative control (nucleoside-free water), and sixteen technical replicates of the non-template control (NTC).

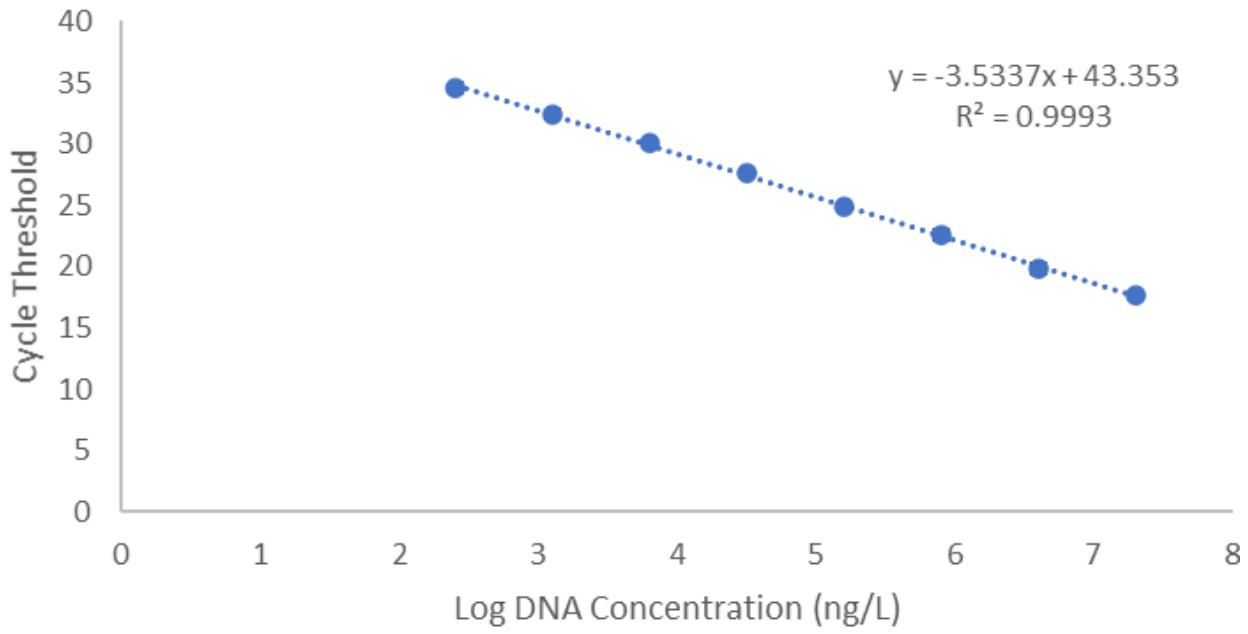

Figure 5. Standard curve equation of relationship between qPCR cycle threshold and log DNA concentration (ng/L) of *X. necrophora* (DMCC2165 and DMCC3828). Each data point represents the mean cycle threshold, quantified from relative fluorescence units (RFU), of *X. necrophora* DNA at a certain concentration (Figure 4). The standard curve equation is $y = -3.5337x + 43.353$, where x = log DNA concentration (ng/L) and y = mean cycle threshold (R^2=0.9993).

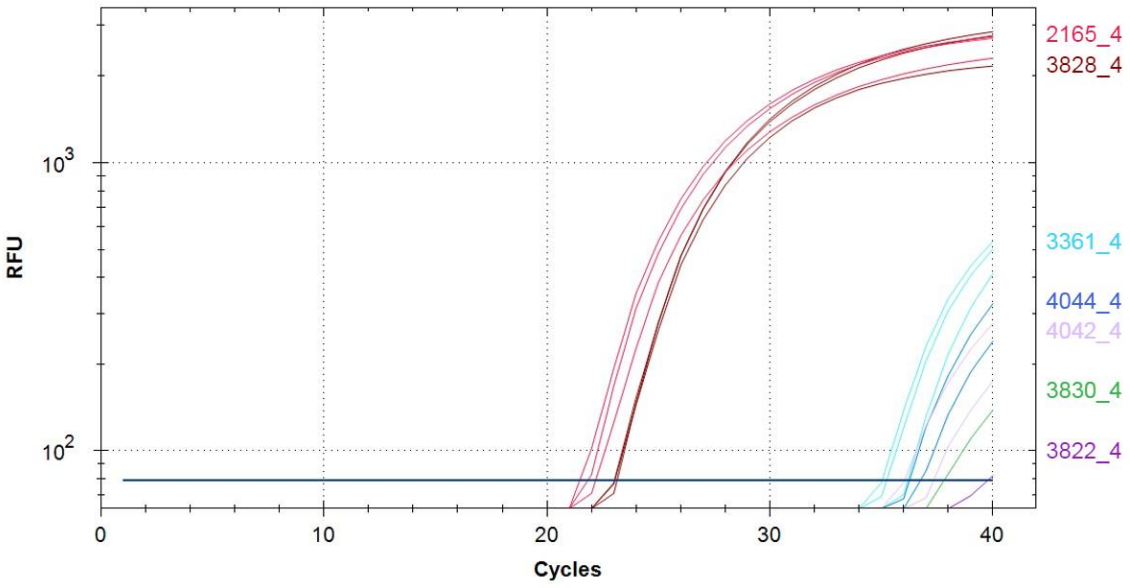

Figure 6. qPCR results from off-target fungal samples (Table 1). Results are depicted as color-coded lines representing relative fluorescence units (RFU) by number of cycles using a log scale. Each label is stylized as isolate_dilution(ng/µL) using a unique color. There were three technical replicates for each positive control (DMCC2165 and DMCC3828), each sample, the negative control (nucleoside-free water), and the non-template control (NTC).

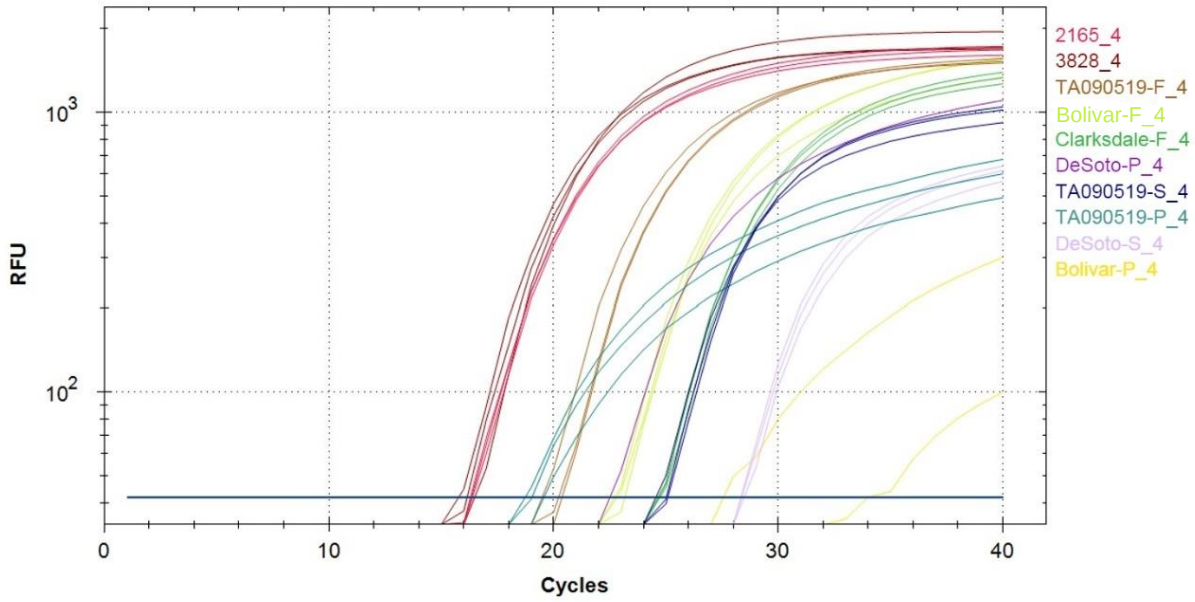

Figure 7. qPCR results from isolates collected in northwestern Mississippi in 2019 (Table 2; Figure 1). DNA was extracted from *X. necrophora* stromata (F), infected plant (P), and soil (S) samples. Results are depicted as color-coded lines representing relative fluorescence units (RFU) by number of cycles using a log scale. Each positive control label is stylized as isolate_dilution (ng/µL) with a unique color. Each sample label is stylized as sample-sampleType_dilution (ng/µL) with a unique color. There were three technical replicates for each positive control (DMCC2165 and DMCC3828), each sample, the negative control (nucleoside-free water), and non-template control (NTC).

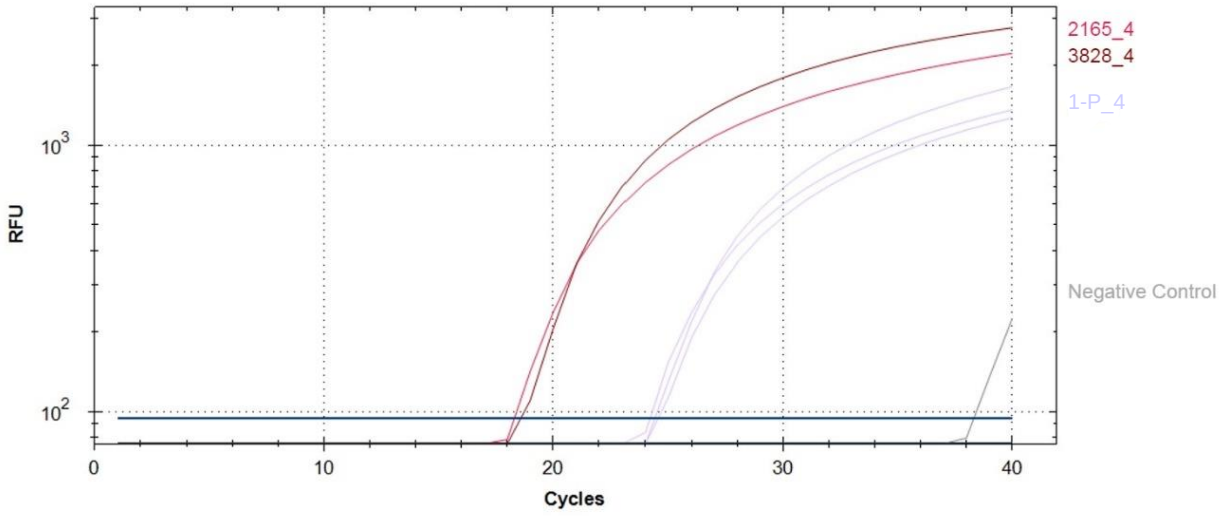

Figure 8. qPCR results from field-obtained soybean plant (P) and soil (S) samples collected in Winnsboro, Louisiana in 2022 (Table 3; Figure 2). Results are depicted as color-coded lines representing relative fluorescence units (RFU) by number of cycles using a log scale. Each positive control label is stylized as isolate_dilution (ng/µL) and each sample label is stylized as sample-sampleType_dilution (ng/µL) with a unique color. There was one technical replicate of each positive control (DMCC2165 and DMCC3828). There were two technical replicates for each soil sample, the negative control (nucleoside-free water), and the non-template control (NTC). There were three technical replicates for each plant sample.

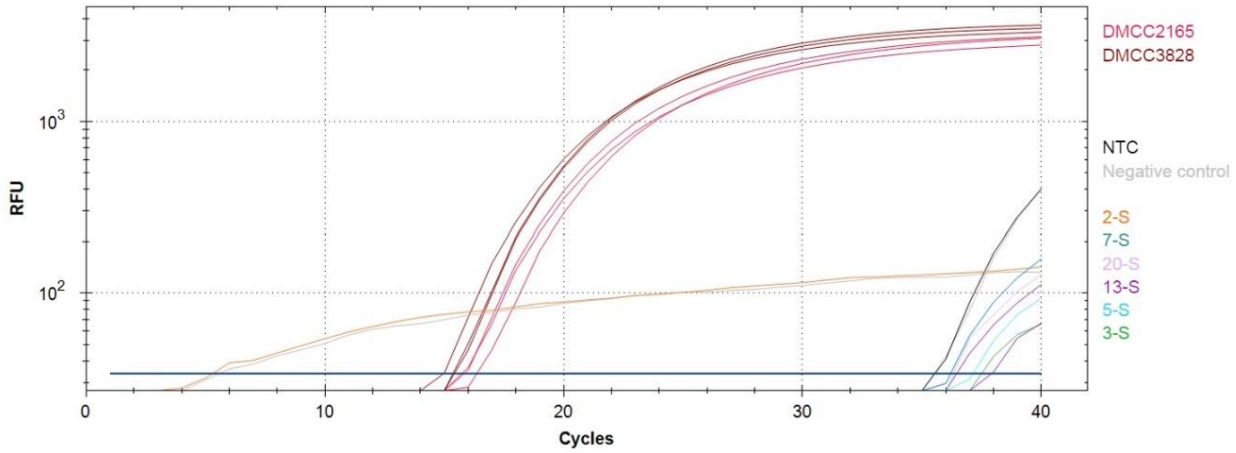

Figure 9. qPCR results from a selection of field-obtained soil (S) samples from Winnsboro without standardizing DNA concentrations (Table 3; Figure 2). The samples tested were: 1-S, 2-S, 3-S, 4-S, 5-S, 6-S, 7-S, 8-S, 11S, 12-S, 13-S, and 20-S. Results are depicted as color-coded lines representing relative fluorescence units (RFU) by number of cycles using a log scale. Each positive control label is stylized as isolate_dilution (ng/µL) and each sample label is stylized as sample-sampleType with a unique color. There were three technical replicates for each positive control (DMCC2165 and DMCC3828), each sample, the negative control (nucleoside-free water), and the non-template control (NTC).

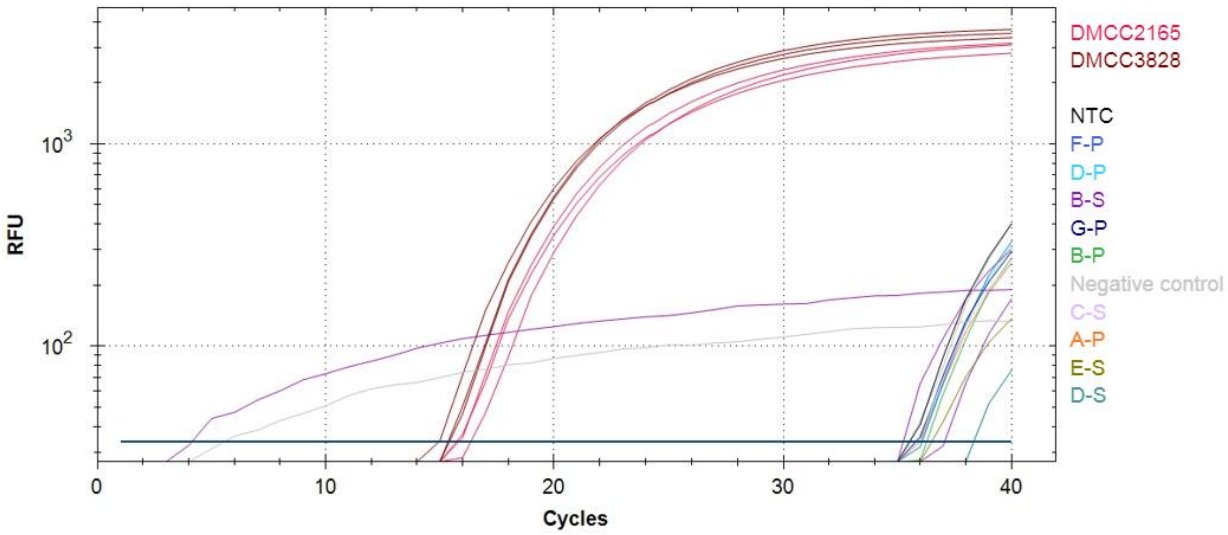

Figure 10. qPCR results from lab-inoculated soybean plant (P) and soil (S) samples. Results are depicted as color-coded lines representing relative fluorescence units (RFU) by number of cycles using a log scale. Each positive control label is stylized as isolate_dilution (ng/µL) and each sample label is stylized as sample-sampleType with a unique color. There were three technical replicates for each positive control (DMCC2165 and DMCC3828), each sample, the negative control (nucleoside-free water), and the non-template control (NTC).